

Detuning control of Rabi vortex oscillations in light matter coupling

Amir Rahmani¹

¹*Department of Physics, Yazd university, Yazd, Iran*

We study analytically the dynamics of vortices in strongly coupled exciton–photon fields in the presence of energy detuning. We derive equations for the vortex core velocity and mass, where they mainly depend on Rabi coupling and the relative distance between the vortex cores in photon and exciton fields, and as the result core positions oscillate in each field. We use Magnus force balanced with a Rabi induced force to show that the core of the vortex behaves as an inertial-like particle. Our analysis reveals that the core is lighter at periphery of the beam and therefore it is faster at that region. While detuning induces oscillations in population imbalance of components through relative phase between coupled fields, in the presence of topological charges detuning can control the orbital dynamics of the cores. Namely, it brings the vortex core to move on larger or smaller orbits with different velocities, and changes angular momentum and energy content of vortex field.

I. INTRODUCTION

The rotation of objects has always been an extremely fascinating and challenging problem. Examples of angular motions are given in classical physics [1, 2] and engineering [3]. When it comes to rotation in a fluid [4], the term “vortex” is used to describe the peculiar motion around a central region. Vortices typically occur in the wake of fluid motion where viscosity is the underlying physical mechanism. To quantify the rotation of a fluid, one can introduce the concept of vorticity, defined as the curl of the velocity field, and circulation, defined as the contour integral of the tangential velocity component. The latter concept is connected to the former (total vorticity) by Stokes’s theorem. In contrast to a conventional fluid that can have arbitrary circulation, a Bose–Einstein condensate (BEC) is constrained to carry quantized circulation. Such a property is on the other hand typical of a complex-valued wavefunction, where the density profile can include a depleted region surrounded by quantized circulations. The flow in a condensate has the intrinsic property of being inviscid, i.e., there is no viscosity to bring the flow to a stop. Mathematically, a condensate with a vortex is not simply-connected and then Stokes’ theorem does not apply. The idea of quantized vortices was introduced for the first time with superfluid Helium, and was then extended to other condensates. Quantized vortices are now commonplace in superconductors [5], superfluids [6], atomic BECs [7], and polariton condensates [8, 9]. Quantized vortices are recognized by a null density region around which the phase wraps itself in quantized units of 2π . Fields with such phase defect carry a quantized orbital angular momentum [10]. In this work, we study vortices in two-component (exciton-photon) condensates, which leads to an interesting interplay for the topology of the fields due to strong coupling (Rabi oscillations) on the one hand and the vorticity on the other hand. Specifically, we will focus on the role of the energy detuning between the exciton and photon components, which is known to result in nontrivial dynamics [11, 12]. For such an investigation, microcavity polaritons [13]—quasiparticles that arise from the strong coupling be-

tween microcavity photon and exciton quantum well—are ideally suited (one could also consider spin-orbit coupled BEC [14, 15]). Polaritons have some interesting attributes. They have a very light effective mass (due to their photonic component), they interact through their excitonic component, and their photon and exciton components can also be easily detuned. The condensed phase of polaritons was reported in 2006 [16] which has initiated an intense followup of fundamental research, including quantum hydrodynamics [17, 18], superfluidity [8, 19], Josephson effects [20], and vortices [8, 21–24], among others. The regime of strong coupling, typically evidenced through the splitting between an upper and a lower polariton branch in the dispersion relation, is more notable for our purpose for the dynamics of Rabi oscillations between the photonic and excitonic components, whose coherent control is now well implemented at the femtosecond level with polaritons [25].

Even fields with no phase defects (vortices) exhibit peculiar dynamical effects in presence of an energy detuning between the components, such as oscillations in their relative phase that result in oscillations in their population imbalance [11, 12]. A particular example is shown in Fig. 1. Here, the population imbalance between the components is given by $\rho \equiv (N_{ph} - N_{ex})/(N_{ph} + N_{ex})$, with N_{ph} and N_{ex} the population for the photon and exciton

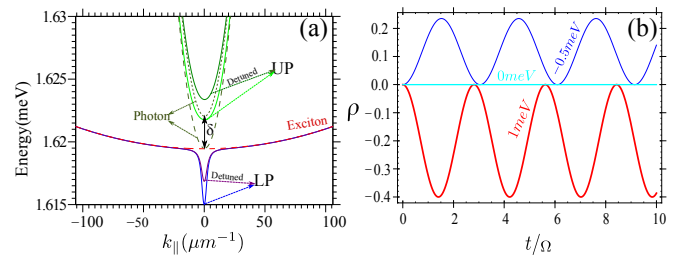


FIG. 1. (a): Polariton dispersion for positive detuning, with an upward shift of the branches. (b): Effect of detuning on the population imbalance $\rho = (N_{ph} - N_{ex})/(N_{ph} + N_{ex})$, for three detuning energies: $\delta = -0.5 meV$ in red, $\delta = 0 meV$ in cyan, and $\delta = 1 meV$ in blue color. Ω is the Rabi frequency.

fields respectively, being initially zero: $N_{ph}(0) = N_{ex}(0)$. For zero energy detuning, there is no oscillations in ρ , although with the imbalance in the initial relative phase of the components there would be oscillation in populations. However, by increasing or decreasing the detuning, some oscillations are triggered. With detuning, the population imbalance takes a nonzero mean value, which increases with detuning; it also changes the frequency of oscillation.

In this work, we study analytically how the vortex dynamics gets affected by detuning in the regime of strong coupling regime. We restrict our analysis to an ideal polariton gas in the Hamiltonian regime, where the Rabi coupling is the predominant interaction that drives the vortex core to move periodically. To describe the core motion, we invoke a Magnus-like force [26, 27] that is balanced by a force which originates from the Rabi coupling. This provides an expression for the inertial mass of the vortex core, which changes in time and is of the order of 10^{-15} kg and 10^{-12} kg, depending on the position of the core. Such a behavior is particular to a polaritonic system, as its binary nature gives the core a time-dependent attribute. Based on our analysis, we demonstrate that the core behaves as an inertial particle, that is, it has a position, a velocity, and a mass. Furthermore, we are dealing with a not-constant mass case. We show that by changing the detuning, the core moves faster or slower, which is the result of a particle transfer between the two coupled fields; then detuning addresses a controlling mechanism on the dynamics of the core. Also, it controls the angular momentum of the field.

The text is organized as follows: Section II presents the relevant theoretical description of polariton BEC based on its photonic and excitonic components. In section III, we describe the oscillation of the core and how it is affected by detuning. In the following section IV, we focus on the effect of detuning on quantum averages. Finally we present concluding remarks in section V.

II. THEORY

The polariton in the exciton-photon basis is an example of a two-component Bose system. The equations of motions for fields in binary Bose system can be conveniently described as quantized fields [28] with the following Hamiltonian:

$$\hat{H} = \frac{\hbar^2}{2m_{ph}} |\vec{\nabla} \psi|^2 + E_{ph} \psi^\dagger \psi + \frac{\hbar^2}{2m_{ex}} |\vec{\nabla} \varphi|^2 + E_{ex} \varphi^\dagger \varphi + \hbar\Omega (\psi^\dagger \varphi + \varphi^\dagger \psi) + \hbar g |\varphi|^4. \quad (1)$$

Here, the two first terms describe the free evolution of the photon (ψ) and exciton (φ) fields, respectively; the first term in the second line describes the *Rabi coupling* between the photon and the exciton fields, which transfers excitations at the Rabi frequency Ω ; the last term

accounts for self-interaction in the exciton field, with $\hbar g$ as the exciton-exciton interaction strength.

A. Main Equations

Based on the Hamiltonian in Eq. (1), the dynamics of 2D interacting polaritons is described by a set of coupled Schrödinger equation and Gross Pitaevskii equation for the photon ψ and exciton φ fields, respectively:

$$i\hbar\partial_t \begin{pmatrix} \psi(x, y, t) \\ \varphi(x, y, t) \end{pmatrix} = \mathcal{L} \begin{pmatrix} \psi(x, y, t) \\ \varphi(x, y, t) \end{pmatrix}, \quad (2)$$

where

$$\mathcal{L} = \begin{pmatrix} -\frac{\hbar^2 \nabla^2}{2m_{ph}} + E_{ph} & \hbar\Omega \\ \hbar\Omega & -\frac{\hbar^2 \nabla^2}{2m_{ex}} + E_{ex} + \hbar g |\varphi|^2 \end{pmatrix}. \quad (3)$$

Here, $m_{ex} = (m_e + m_h)m_0$ stands for the exciton mass and $m_{ph} \approx n\pi\hbar/(cl_c) = (n^2/c^2)(E_x + \delta)$ is the effective photon mass, with $E_{ph} \approx \hbar c\pi/(nl_c)$ where l_c is the microcavity length. E_{ex} is the exciton energy that is given by $E_{ex} = 13.6 \text{ eV} \frac{\mu}{m_0 n}$, where μ is the reduced effective mass of the exciton and m_0 is the bare electron mass. For later calculations, we may need equations in a rescaled form, then one can rescale the units of time and length as $t \rightarrow t\Omega$, $x \rightarrow x/\xi$, $y \rightarrow y/\xi$, $k_x \rightarrow k_x \xi$, and $k_y \rightarrow k_y \xi$ where $\xi \equiv \sqrt{\hbar/\Omega m_{ph}}$.

Theoretical works [29] have estimated the self-interaction strength as $\hbar g \approx 6E_x a_B^2$, where a_B is the exciton Bohr radius. Calculating $\hbar g/(\hbar^2/2m_p)$, with $m_p \approx 10^{-4}m_0$ as the polariton mass, one finds that polaritons are in the regime of weak interactions. However, experimental evidence [30, 31] has recently suggested that the interaction constant $\hbar g$ could be of the order of several meV μm , which puts polaritons in the regime of strong self-interaction. In this work, we aim at considering the effect of energy detuning on the dynamics of coupled fields with phase defects, with an emphasis on the role of the Rabi coupling as opposed to polariton-polariton interactions. Such a regime of vortex dynamics has been reported recently in Ref. [9], which seems to justify the realm of a linear dynamics of coupled fields; therefore, hereafter, we ignore the effect of self-interaction energy in our calculations.

B. Initial states

Our objective here is to study the dynamics of vortices in the regime of strong coupling. To this aim we

introduce vortices in the initial condition as follows:

$$\psi_0 \equiv \psi(x, y, t = 0) = \frac{e^{-(x^2+y^2)/2w^2}}{w\sqrt{\pi(w^2 + |z_c(0, 0, 0)|^2)}} z_c(x, y, 0), \quad (4a)$$

$$\varphi_0 \equiv \varphi(x, y, t = 0) = \frac{e^{-(x^2+y^2)/2w^2}}{w\sqrt{\pi(w^2 + |z_x(0, 0, 0)|^2)}} z_x(x, y, 0), \quad (4b)$$

where $z_j(x, y, t) = x - x_j(t) + i(y - y_j(t))$ with $j = \{c, x\}$. Here, each field is normalized. The parameter w control the Gaussian spot size. It is worth mentioning that one can consider coupled fields with different topological charge in each, however, we found out that the initial states (4) are the simplest choice to illustrate the physics we want to discuss. Also, note that an initial condition with a vortex in the photon field only does not develop any dynamics for the vortex core.

III. OSCILLATION OF THE CORE

In this section we discuss the solutions of equation (2) when $\Omega = 0$. Despite the fact that the equations are

linear, we will see that the solutions are not trivial.

A. Approximate Solution

There is no closed-form solution for Eq. (2) even in the absence of a nonlinear term. However, one can find approximate solutions through a series expansion, for example, by employing spectral methods [32] or homotopy analysis methods [33]. In this text, we use a spectral method, with the Hermite $H_n(x)$ functions as basis functions; thus, we expand the wavefunctions $\psi(x, y)$ and $\varphi(x, y)$ as:

$$\psi(x, y) = \sum_{n,m=0} u_{n,m}(x, y) a_{n,m}(t), \quad (5a)$$

$$\varphi(x, y) = \sum_{n,m=0} u_{n,m}(x, y) b_{n,m}(t), \quad (5b)$$

where we introduce the basis functions $u_{n,m}(x, y)$ as:

$$u_{n,m}(x, y) = c_{n,m} H_n(x/w) H_m(y/w) e^{-(x^2+y^2)/(2w^2)}, \quad (6)$$

with $c_{n,m} = \frac{1}{w\sqrt{\pi 2^{n+m} \Gamma(n+1) \Gamma(m+1)}}$. Here, $\Gamma(n)$ stands for the gamma function. The coefficients $a_{n,m}$ and $b_{n,m}$ satisfy the following initial-value differential equations:

$$i\hbar \frac{da_{n,m}}{dt} = -\frac{\hbar^2}{2m_c w^2} \left(-(1+n+m)a_{n,m} + \frac{\sqrt{(n+1)(n+2)}}{2} a_{n+2,m} + \frac{\sqrt{(m+1)(m+2)}}{2} a_{n,m+2} \right. \\ \left. + \sqrt{n(n-1)} a_{n-2,m} + \sqrt{m(m-1)} a_{n,m-2} \right) + \hbar \Omega b_{n,m} + E_c a_{n,m}, \quad (7a)$$

$$i\hbar \frac{db_{n,m}}{dt} = -\frac{\hbar^2}{2m_x w^2} \left(-(1+n+m)b_{n,m} + \frac{\sqrt{(n+1)(n+2)}}{2} b_{n+2,m} + \frac{\sqrt{(m+1)(m+2)}}{2} b_{n,m+2} \right. \\ \left. + \sqrt{n(n-1)} b_{n-2,m} + \sqrt{m(m-1)} b_{n,m-2} \right) + \hbar \Omega a_{n,m} + E_x b_{n,m}. \quad (7b)$$

These provide an infinite hierarchy of equations, coupled by the Rabi and kinetic energy terms. One way to truncate this hierarchy is to note that for $w^2 \gg \xi^2$, only those $a_{n,m}$ and $b_{n,m}$ that have nonzero initial values are several orders larger than the other coefficients with zero initial values; it is the case when w is of the order of several micrometers, which is a typical estimate found in experimental reports [9]. Then, we can approximate the wavefunctions as:

$$\psi(x, y, t) \cong a_{00}(t) u_{00} + a_{1,0}(t) u_{1,0} + a_{0,1}(t) u_{0,1}, \quad (8a)$$

$$\varphi(x, y, t) \cong b_{00}(t) u_{00} + b_{1,0}(t) u_{1,0} + b_{0,1}(t) u_{0,1}. \quad (8b)$$

The equations for $a_{0,0}(t)$, $a_{0,1}(t)$, $a_{1,0}(t)$, $b_{0,0}(t)$, $b_{0,1}(t)$ and $b_{1,0}(t)$ are given in Appendix A.

B. Dynamics of the core

Examples of solutions for zero detuning are shown in Fig. 2. The cores are initially located at $(x_c(0) = -aw, y_c(0) = 0)$ in the photon field and at $x_x(0) = 0, y_x(0) = 0$ in the exciton field. While they move periodically on their orbits, the background densities oscillate similarly. Here, the fields are initially normalized and remain so in time. This implies that there is no particle exchange between the coupled fields, however, background densities are oscillating while the core moves. The motion of the core is induced by the presence at a distance of the other core, by the local density of the other field, and by the Rabi coupling. The combined effect is that the vortex core moves with a non-constant speed.

We now explain the dynamics based on our main equa-

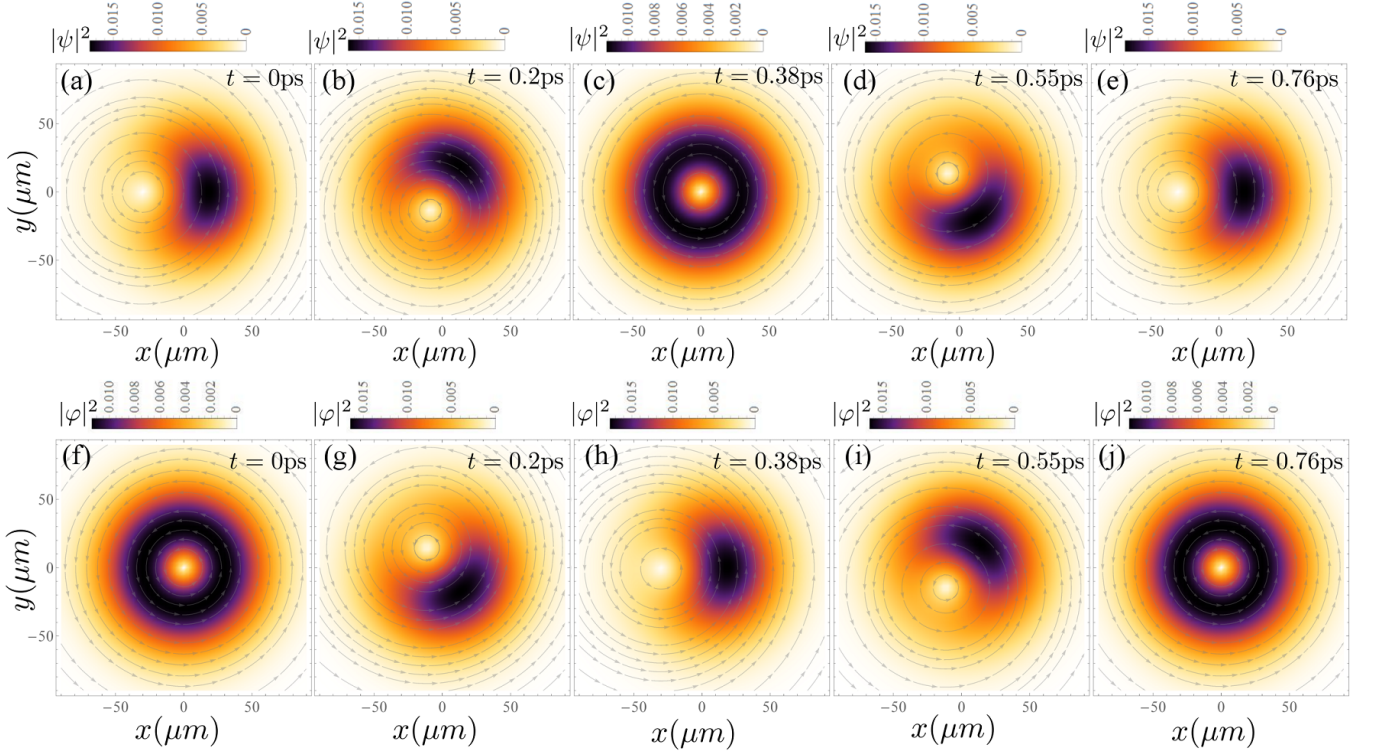


FIG. 2. Oscillation of the core in the photon (upper panels) and in the exciton (lower panels) fields, shown for one period of motion. The wavepacket is initially normalized to one and the energy detuning is zero, which implies no particle exchange between the two fields, which remain normalized in time. Each fields carries a winding number of $l = 1$. The photon field is initially deformed by displacing the core to a position far from the origin, while the core in the exciton field is located at the origin. For the dynamics, the local density oscillates similarly. The core does not move with a constant speed. We also show the stream lines of superfluid velocity for each field, as circles centered on the vortex core position. Here, we used: $\hbar\Omega = 2.75\text{meV}$, $a = 1.2$, $w = 25\mu\text{m}$.

tions. One notes that the core in each field never disappears completely, which implies that the solutions can be written as the product of a background density and a complex time-dependent function $z_j(t) = x - x_j(t) + i(y - y_j(t))$ for depleted points in the fields, as we have:

$$\psi = \rho_{ph}(x, y, t) e^{i\phi_{ph}(x, y, t)} z_c(t), \quad (9a)$$

$$\varphi = \rho_{ex}(x, y, t) e^{i\phi_{ex}(x, y, t)} z_x(t). \quad (9b)$$

By adding them in Eq. (2) one can find two central equations for the core velocities:

$$\begin{aligned} \mathbf{v}_c = & \frac{\hbar}{m_{ph}} (\vec{\nabla} \phi_{ph} - \hat{k} \times \vec{\nabla} \ln \rho_{ph})|_{x=x_c, y=y_c} \\ & + \Omega \frac{\rho_{ex}}{\rho_{ph}} (\hat{j} \Delta \mathbf{r} \cdot \hat{S}_+ + \hat{i} \hat{k} \times \Delta \mathbf{r} \cdot \hat{S}_+), \end{aligned} \quad (10a)$$

$$\begin{aligned} \mathbf{v}_x = & \frac{\hbar}{m_{ex}} (\vec{\nabla} \phi_{ex} - \hat{k} \times \vec{\nabla} \ln \rho_{ex})|_{x=x_x, y=y_x} \\ & - \Omega \frac{\rho_{ph}}{\rho_{ex}} (\hat{j} \Delta \mathbf{r} \cdot \hat{S}_- + \hat{i} \hat{k} \times \Delta \mathbf{r} \cdot \hat{S}_-), \end{aligned} \quad (10b)$$

where $\Delta \mathbf{r} = \mathbf{r}_c - \mathbf{r}_x$ gives the relative vector-position of the cores, and $\hat{S}_{\pm} = \cos(\phi_{ph} - \phi_{ex})\hat{i} \pm \sin(\phi_{ph} -$

$\phi_{ex})\hat{j}$. These equations have the same mathematical form even in the presence of self-interactions and external potentials, although with a potential the dynamics of the cores take a different nature. Also, we note that there are three factors that determine the variation of velocities in time; one factor depends on the distance between the cores in each field which is followed by the Rabi frequency Ω . The other two factors depend on the gradient of the local phase and density of each field; these two factors come from the kinetic energy through a dependency on $\hbar/m_{ph,ex}$. Comparing $\hbar/m_c w$ and Ωw to approximate the order of the factors that define the cores velocity, we assume, based on experimental evidences, that $\Omega \gg \hbar/m_c w^2$, which implies that the Rabi-induced velocity is the dominating factor for the motion of the vortex core. For $\Omega = 0$, each field turns to a free field, and there is no motion of the core. In our case, there is no external potential, and the motion of the core is mediated only by the interplay between the Rabi coupling and the topology of the deformed field when a core is displaced to a point far from the center of the field. As the core is moving on a curved path, it has an angular

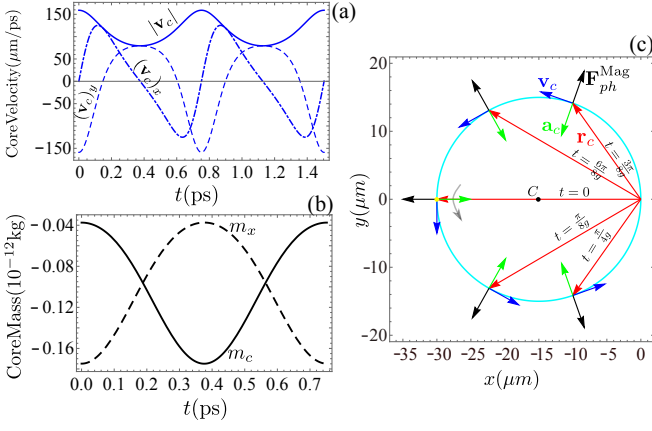


FIG. 3. (a): absolute value of core velocity $|\mathbf{v}_c|$ (solid line in blue) in the photon field at zero detuning. We also show its components $(\mathbf{v}_c)_x$ (dashed line) and $(\mathbf{v}_c)_y$ (dot-dashed line). The core is faster when it is the farthest from the origin. (b): trajectory (in cyan) of the core (yellow point) in the photon field. Position vector (in red), velocity vector (in blue), acceleration vector (in green), and Magnus force vector (in black) are shown for different times. The acceleration vector points toward the center C (black point). The Magnus force points in the opposite direction. (c) shows the core mass in the photon (solid line) and exciton (dashed line) fields. The core is heavier at the origin. For numerical calculation, we used the same parameter as Fig. (2).

velocity $\vec{\omega}$ which is given by:

$$\vec{\omega}_j = \frac{\mathbf{r}_j \times \mathbf{v}_j}{x_j^2 + y_j^2}, \quad (11)$$

with $j = \{c, x\}$ and \mathbf{r}_j denoting the position vector of the core in the photon ($j = c$) and in the exciton ($j = x$) fields.

At this stage, we have shown that a core has both a linear and angular velocity, and its kinematic (description of the motion itself with no reference to the underlying forces) is thus transparent. To address the kinetics (descriptions of the causes of motions) of the core, however, we also need to refer to the force that acts on it. In a classical fluid, the circulation of a vortex can influence any other vortex at a distance, which results in an effective force perpendicular to the velocity of the vortex core[34]. Bringing this picture to a quantum fluid, it was shown that such a force is connected to the gradient of the total energy of the system for a BEC in an harmonic trap[35, 36], and ambiguously for two unbounded coupled BECs[34] in the nonlinear regime. For polaritons in the linear regime, one can show that the predominant energy-scale in the system is the Rabi energy, defined as:

$$E_R(x_c, y_c, x_x, y_x) \equiv 2\hbar\Omega\text{Re}\langle\psi|\varphi\rangle, \quad (12)$$

and this depends on the positions of the vortex cores. Taking the gradient with respect to the core positions, one can introduce a force through $\mathbf{F}^R \equiv -\vec{\nabla}E_R$. For

a core in the photon field, the x and y components of this force have a linear dependency on x_x, y_x through an equation like $\Omega(\alpha_1(t)x_x + \alpha_2(t)y_x)$, while for a core in the exciton field, it behaves like $\Omega(\beta_1(t)x_c + \beta_2(t)y_c)$, where α_i and β_i are some real coefficients depending on the parameters of the system. On the other hand, there would be a Magnus-like force that depends on the velocity of the vortex core. To find this, we multiply velocities in Eqs. (10) from the left respectively by $-2\pi\hbar\rho_{ph}\hat{k}$ and $-2\pi\hbar\rho_{ex}\hat{k}$, and we find:

$$\mathbf{F}_{ph}^{\text{Mag}} + \mathbf{F}_{ph}^{\text{Rabi}} = \mathbf{F}_{ph}^{\text{Kin}}, \quad (13a)$$

$$\mathbf{F}_{ex}^{\text{Mag}} + \mathbf{F}_{ex}^{\text{Rabi}} = \mathbf{F}_{ex}^{\text{Kin}}, \quad (13b)$$

where we introduce the following expressions; for the core in the photon field:

$$\mathbf{F}_{ph}^{\text{Mag}} = -\rho_{ph}\mathbf{K}_{ph} \times (\mathbf{v}_c - \frac{\hbar}{m_{ph}}\vec{\nabla}\phi_{ph}), \quad (14a)$$

$$\mathbf{F}_{ph}^{\text{Kin}} = -\frac{\hbar\rho_{ph}}{m_{ph}}\mathbf{K}_{ph} \times (\hat{k} \times \vec{\nabla}\ln\rho_{ph}), \quad (14b)$$

$$\mathbf{F}_{ph}^{\text{Rabi}} = \Omega\rho_{ex}\mathbf{K}_{ph} \times (\hat{j}\Delta\mathbf{r} \cdot \hat{S}_- + \hat{i}\hat{k} \times \Delta\mathbf{r} \cdot \hat{S}_-), \quad (14c)$$

and for the core in the exciton field:

$$\mathbf{F}_{ex}^{\text{Mag}} = -\rho_{ex}\mathbf{K}_{ex} \times (\mathbf{v}_x - \frac{\hbar}{m_{ex}}\vec{\nabla}\phi_{ex}), \quad (15a)$$

$$\mathbf{F}_{ex}^{\text{Kin}} = -\frac{\hbar\rho_{ex}}{m_{ex}}\mathbf{K}_{ex} \times (-\hat{k} \times \vec{\nabla}\ln\rho_{ex}), \quad (15b)$$

$$\mathbf{F}_{ex}^{\text{Rabi}} = -\Omega\rho_{ph}\mathbf{K}_{ex} \times (\hat{j}\Delta\mathbf{r} \cdot \hat{S}_+ + \hat{i}\hat{k} \times \Delta\mathbf{r} \cdot \hat{S}_+), \quad (15c)$$

where $\mathbf{K}_j = 2\pi\hbar\hat{k}$. Here, we have a balance between the Magnus force $\mathbf{F}_j^{\text{Mag}}$ added to a Rabi mediated force $\mathbf{F}_j^{\text{Rabi}}$ and a gradient force $\mathbf{F}_j^{\text{Kin}}$. The latter force has an origin in quantum kinetic energy or zero point energy, and is related to the quantum pressure. Examining the orbital motion of the core, as it is shown in Fig. (2), one can conclude that a possible force that makes the core drift should depend on the relative distance between the cores, as when $x_c(0) = x_x(0)$ and $y_c(0) = y_x(0)$ there is no motion for the core. This implies that any effective force \mathbf{F}^R related to the gradient of the Rabi energy does not reproduce the expected dynamics of the vortex core in our binary system.

Based on the above equations for the forces, we now have a better understanding for an effective mass associated to the core. To this end, we note that the application of a force normal to the velocity direction does change the linear momentum of an object, and the rate of the change in momentum is equal to the applied force. This implies that there would be a rotational acceleration related to the cross product of the linear and angular velocities, which in the case of the core motion results in

$$\mathbf{F}_c \equiv m_c\vec{\omega}_c \times \mathbf{v}_c = -\rho_{ph}\mathbf{K}_{ph} \times \mathbf{v}_c, \quad (16a)$$

$$\mathbf{F}_x \equiv m_x\vec{\omega}_x \times \mathbf{v}_x = -\rho_{ex}\mathbf{K}_{ex} \times \mathbf{v}_x, \quad (16b)$$

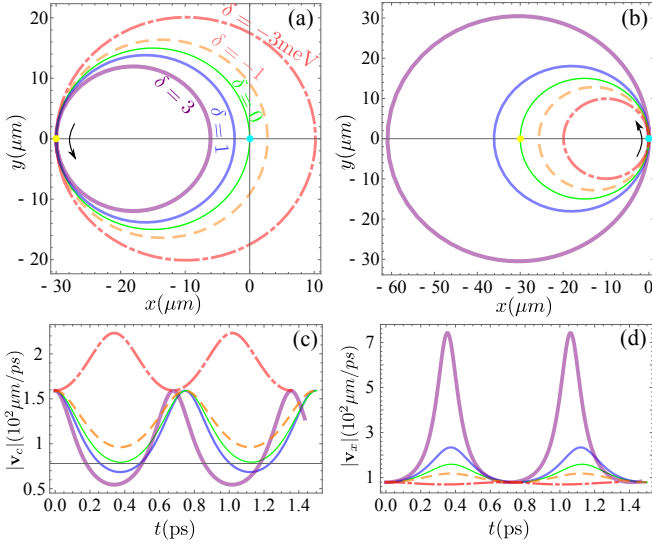


FIG. 4. (a) and (b) show orbits for the core oscillations for different energy detuning between the photon and exciton fields. The core in the photon field is shown as a yellow point, and in the exciton field as a green point. In (a) and for positive (negative) detuning, the core moves on smaller (larger) orbits, and its dynamical properties are different. It opposite happens for the core in the exciton field. The amplitude of velocity ($|\mathbf{v}_c|$ and $|\mathbf{v}_x|$) are shown in (c) and (d). As the core takes larger orbits, it speeds up even up to speeds larger than the speed of light.

where m_c and m_x are the core masses in the photon and exciton fields, respectively, and we have:

$$m_c = -\frac{2\pi\hbar\rho_{ph}(x_c, y_c)}{\omega_c}, \quad (17a)$$

$$m_x = -\frac{2\pi\hbar\rho_{ex}(x_x, y_x)}{\omega_x}, \quad (17b)$$

which depend explicitly on the angular velocity of the cores. As there is no dependency on the Rabi frequency, one can be hopeful that even in the presence of self-interaction or external potentials, the equations for the masses m_c and m_x will have the same mathematical form, and that any effects associated with interactions and potential will be collected in angular frequencies of the cores and ambient densities.

Now we have a complete description for the core dynamics with its position, velocity, mass and force associated to the core. In Fig. 3, we show examples of the dynamical variables for zero detuning and for the photon field. The core is initially located at $(-aw, 0)$, as is indicated by the yellow point in Fig. 3(a). While the core moves counter-clockwise, its speed $|\mathbf{v}_c|$ decreases to a minimum, when the core finds itself at the origin, and then the core speeds up as it approaches to its initial position. With such a variation in its speed, the core decelerates in the first half of its motion and then accelerates in the rest of its motion. The acceleration vector is pointed

toward a point C inside the orbit, while the Magnus force is pointed in the opposite direction. This implies a negative mass for the core, which is shown in Fig. 3(b) for one period of motion. The core is lighter when it take its position at the periphery of the local density. Since in our system, there is no external potential, such a variation in the inertial mass of the core originates exclusively from the binary nature of the fields. Certainly, with the presence of an external potential and/or self-interactions, the core mass would behave differently, depending on the interplay between the Rabi energy and the other energy scales of the system.

Now we turn to consider the effect of the energy detuning. We first study the orbital motions of the cores for different detunings, which are shown in Fig. 4(a) and (b) for the photon and exciton fields, respectively. With a nonzero detuning, the cores move on different orbits, while for a zero detuning, they orbit on the same path. Negative and positive detunings have different effects, as the cores can move on smaller or larger orbits. Figures 4(c) and (d) show the corresponding amplitudes of velocities: $|\mathbf{v}_c|$ and $|\mathbf{v}_x|$. As the detuning has opposite effects in the photon and exciton fields, it decreases or increases the core speeds. It seems, as predicted in [9], that the core speed could increase even to value larger than the speed of light $c = 3 \times 10^2 \mu\text{m}/\text{ps}^{-1}$, and at the same time, there would be a decrease of its mass. An angular momentum (AM) polariton state $|\Psi\rangle = \alpha|\psi\rangle_{l_c} + \beta|\varphi\rangle_{l_x}$, where $|\psi\rangle_{l_c}$ and $|\varphi\rangle_{l_x}$, respectively, indicate photon and exciton states with different topological charges l_c and l_x , will propagate with a group velocity that depends on the topology of the fields. One could expect that by increasing and/or decreasing the detuning and equivalently manipulating the core speed, the group velocity will increase or decrease correspondingly. This controlling over group velocity has practical importance in quantum memory[37].

IV. ANGULAR MOMENTUM AND ENERGY CONTENTS

A wavepacket with a phase defect that results in a rotation of the fluid around a vortex core, has a nonzero value of angular momentum. Namely, the average angular momentum of the wavepacket Ψ is given by

$$\langle \hat{L}_z \rangle = -i\hbar \int r dr d\phi \langle \Psi | \frac{\partial}{\partial \phi} | \Psi \rangle, \quad (18)$$

with $r = \sqrt{x^2 + y^2}$ and $\phi = \arg(x + iy)$ in polar coordinates. For the initial wavepackets in Eqs. (4), one can find $\langle \hat{L}_z \rangle_{ph}(t=0) = \hbar w^2/(w^2 + |z_c|^2)$, and $\langle \hat{L}_z \rangle_{ex}(t=0) = \hbar w^2/(w^2 + |z_x|^2)$, respectively, for the photon and exciton fields; then, with $z_c \neq z_x$, corresponding to placing the cores in different points in space, there is a nonzero initial imbalance for the angular momentum $\Delta l \equiv \langle \hat{L}_z \rangle_{ph} - \langle \hat{L}_z \rangle_{ex} \neq 0$. This also changes

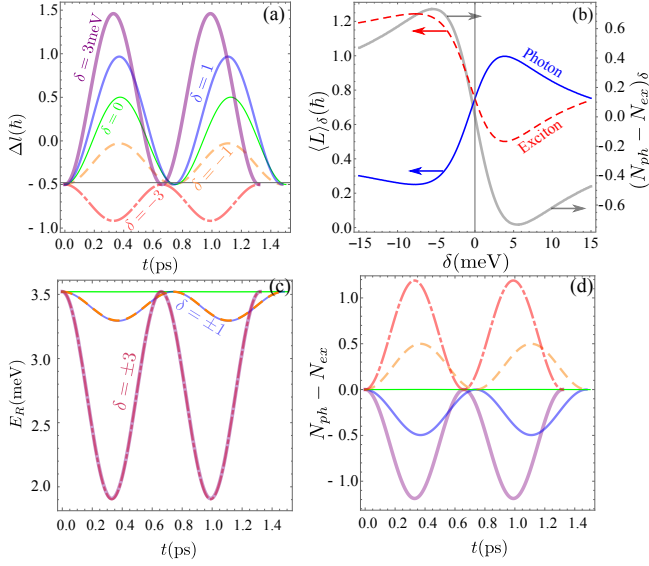


FIG. 5. (a) shows the imbalance in angular momentum: $\Delta l = \langle L_z \rangle_{ph} - \langle L_z \rangle_{ex}$. For positive detuning, the angular momentum of the photon field is larger. We see variations in the period of oscillations with detuning. It is shown for $\delta = 3$ meV in purple, $\delta = 1$ meV in blue, $\delta = 0$ meV in green, $\delta = -1$ meV in orange, and $\delta = -3$ meV in red. (b) The mean value of the angular momentum for the photon (blue—solid line) and exciton (red—dashed line) fields. For negative detunings, the angular momentum is carried mostly by the photon field. The mean value of the population imbalance is also shown (in dark—thick solid line). In (c) we present the variations of the Rabi energy in time for different detuning. In (d) we show population imbalance.

the energy content of the coupled fields. To study this, we first note that the kinetic energy is of the order of $\hbar\Omega/2w^2$ for the photon field and of $(m_{ph}/m_{ex})\hbar\Omega/2w^2$ for the exciton field; and that for w equal to several ξ , these are at least two orders less than the Rabi energy which is proportional to $\hbar\Omega$. This means that one can neglect the kinetic energy for w in the range of several ξ . For zero detuning, the Rabi energy is a constant of motion and is given at $t = 0$ by $E_R(t = 0) = 2\hbar\Omega(w^2 + \mathbf{r}_c \cdot \mathbf{r}_x) / \sqrt{(w^2 + |z_c|^2)(w^2 + |z_x|^2)}$. The configuration with $\mathbf{r}_c = \mathbf{r}_x$ is unstable to a displacement of the cores, since by increasing the distance between the two cores, the energy of the system decreases correspondingly. One can deduce that states with cores at a distance are more favorable than $\mathbf{r}_c = \mathbf{r}_x$, corresponding to fields being at rest, and this decreasing in energy as well as inducing the nonzero Δl , will be realized through the rotation of the vortex cores.

We now describe the time evolution of the energy and angular momentum in Fig. 5 for some negative and positive detuning. One can see in Fig. 5(a) the time evolution of Δl . There will be an exchange of the angular momentum between the components of the coupled fields, which is periodic in time, as we expect from the

Rabi nature of the coupling. By placing the photon vortex core at a distance to the exciton vortex core, there exists a nonzero (here, negative) initial imbalance in angular momentum, as the photon part has initially less rotational content than the exciton part, and since the total angular momentum should be constant, this imbalance triggers oscillations in the angular momentum. Depending on the energy detuning, there will be oscillations with different periods and behaviors. First we see that by increasing the detuning, there is a decrease in the period of oscillations; then, we see that for positive detuning, there will be longer time intervals with positive imbalance in angular momentum, i.e., the photon field has more angular content in average. On the other hand, with a negative detuning, there would be a state with always $\Delta l < 0$ in time, which implies that the rotational content of the photon field is always less than the exciton field. In this case, the core will be faster in the photon field, as it is being pushed to the periphery of the beam, while the core in the exciton field is slower (see Fig. 4). For an object with a positive mass, one expects that increasing the angular momentum will make it go faster, however, in the case of a vortex core, the opposite happens. Actually, a core is an absence of matter, and it has a negative mass, which results in it being pushed toward regions of low density. It is shown in part (d) in Fig 5, that for a negative detuning, the photon field has more population, and indeed the field has a higher density in the central region, which finally pushes the core, with its negative mass, to the lower density region, i.e., at the periphery of the wavepacket. In part (b), we show the mean value of the angular momentum (right y axis) and of the population imbalance (left y axis). For positive detuning, the population is concentrated in the exciton side and at the same time the photon field has more angular momentum. The reverse happens for negative detuning. One notes that, while the mean value of the population imbalance is symmetric with respect to detuning variations, it is not the case for the angular momentum. It makes the negative detuning a special case for the dynamics of the vortex core. Indeed, if we imagine $\mathbf{r}_c = (-aw, 0)$ and $\mathbf{r}_x = (0, 0)$, one can show that for $\delta \approx -\hbar\Omega(a^2w^2 + \sqrt{1+a^2})/w^2\sqrt{1+a^2}$, there is no evolution of the angular momentum in time, i.e., $\Delta l = \text{const.}$ The total energy of the system $E_T \approx E_R(t) + \delta N_{ph}(t)$ also changes with detuning, although it is a constant of motion, i.e., it does not change with time. Increasing $|\Delta \mathbf{r}|$ and applying detuning, one can set the energy of the system to a desired value. We present the time evolution of the Rabi energy in part (c). Here, as we mentioned before, there is no oscillation in time for zero detuning, due to the zero imbalance in population and the normalization of the wavepackets. Nonzero detuning will however induce oscillations of the Rabi energy. To understand this, we first note that $\partial_t E_R \propto -\delta \text{Im}\langle \psi | \varphi \rangle$ and $\partial_t \text{Im}\langle \psi | \varphi \rangle \propto \delta E_R$; then as $E_R(t = 0)$ is nonzero, and any nonzero detuning will affect $\langle \psi | \varphi \rangle$, and therefore there is an oscillation in the relative phase $\arg[\langle \psi | \varphi \rangle]$, which

drives the population imbalance; hence, a nonzero detuning induces self-trapping for both the population and the angular content of the coupled fields.

V. CONCLUSION

In conclusion, we have studied the dynamics of vortices in coupled exciton-photon fields, where the binary nature of the coupling fields sets the vortex cores in motion. We found out that the vortex core behaves like particles that can be described by their position, velocity and mass. We identified the later based on the Magnus force. Then, we showed the effect of energy detuning to control the dynamics of the vortex core. This provides a control over both the kinematic (positions & velocities) and kinetics (energy & angular momentum) of the field plus the core positioned in the field. This control over the vortex dynamics, that is special for polaritonic system, can have applications in many fields related to angular momentum in matter and light, in particular, for memory reading and writing [37–39] and information processing with angular momentum[40]. It also could be used for manipulating and maintaining vortices in superconductor phases[5, 41].

Appendix A: Details for Equations 8

We mentioned in the main text that the equations of motions for $a_{n,m}$ and $b_{n,m}$ provide a general hierarchy. To solve such systems of ordinary equations, one needs to truncate them based on some criterion. We found that when w is several orders larger than ξ , we can approximate the solutions by keeping those terms that are initially nonzero, while removing other terms due to their small values. Our initial conditions in subsection IIB give the following values for nonzero coefficients in $t = 0$:

$$a_{0,0}(0) = \frac{-(x_c + iy_c)}{\sqrt{w^2 + |z_c(0, 0, 0)|^2}}, \quad (\text{A1a})$$

$$a_{0,1}(0) = \frac{w\sqrt{2}}{2\sqrt{w^2 + |z_c(0, 0, 0)|^2}}, \quad (\text{A1b})$$

$$a_{1,0}(0) = \frac{iw\sqrt{2}}{2\sqrt{w^2 + |z_c(0, 0, 0)|^2}}, \quad (\text{A1c})$$

$$b_{0,0}(0) = \frac{-(x_x + iy_x)}{\sqrt{w^2 + |z_x(0, 0, 0)|^2}}, \quad (\text{A1d})$$

$$b_{0,1}(0) = \frac{w\sqrt{2}}{2\sqrt{w^2 + |z_x(0, 0, 0)|^2}}, \quad (\text{A1e})$$

$$b_{1,0}(0) = \frac{iw\sqrt{2}}{2\sqrt{w^2 + |z_x(0, 0, 0)|^2}}, \quad (\text{A1f})$$

which yield the following relations:

$$a_{0,0}(t) = \frac{1}{g_c} e^{-\frac{it}{4w^2}(\Omega(1+m_r)+2(E_{ph}+E_{ex})w^2)} \left(-i(a_{0,0}(0)\Omega + 2w^2(a_{0,0}(0)\frac{\delta}{\hbar} + 2b_{0,0}(0)\Omega)) \sin(\frac{\Omega ct}{4w^2}) + a_{0,0}(0)g_c \cos(\frac{\Omega ct}{4w^2}) \right), \quad (\text{A2a})$$

$$a_{1,0}(t) = \frac{1}{g_d} e^{-\frac{it}{2w^2}(\Omega(1+m_r)+2(E_{ph}+E_{ex})w^2)} \left(-i \sin(\frac{\Omega dt}{2w^2})(a_{1,0}(0)(\Omega + \frac{\delta}{\hbar}w^2) + 2\Omega w^2 b_{1,0}(0)) + a_{1,0}(0)g_d \cos(\frac{\Omega dt}{2w^2}) \right), \quad (\text{A2b})$$

$$a_{0,1}(t) = \frac{1}{g_d} e^{-\frac{it}{2w^2}(\Omega(1+m_r)+2(E_{ph}+E_{ex})w^2)} \left(-i \sin(\frac{\Omega dt}{2w^2})(a_{0,1}(0)(g + \frac{\delta}{\hbar}w^2) + 2\Omega w^2 b_{0,1}(0)) + a_{0,1}(0)g_d \cos(\frac{\Omega dt}{2w^2}) \right), \quad (\text{A2c})$$

$$b_{0,0}(t) = \frac{1}{g_c} e^{-\frac{it}{4w^2}(\Omega(1+m_r)+2(E_{ph}+E_{ex})w^2)} \left(i(b_{0,0}(0)\Omega + 2w^2(b_{0,0}(0)\frac{\delta}{\hbar} - 2a_{0,0}(0)g)) \sin(\frac{\Omega ct}{4w^2}) + b_{0,0}(0)g_c \cos(\frac{\Omega ct}{4w^2}) \right), \quad (\text{A2d})$$

$$b_{1,0}(t) = \frac{1}{g_d} e^{-\frac{it}{2w^2}(\Omega(1+m_r)+2(E_{ph}+E_{ex})w^2)} \left(i \sin(\frac{\Omega dt}{2w^2})(b_{1,0}(0)(\Omega + \frac{\delta}{\hbar}w^2) - 2\Omega w^2 a_{1,0}(0)) + b_{1,0}(0)g_d \cos(\frac{\Omega dt}{2w^2}) \right), \quad (\text{A2e})$$

$$b_{0,1}(t) = \frac{1}{g_d} e^{-\frac{it}{2w^2}(\Omega(1+m_r)+2(E_{ph}+E_{ex})w^2)} \left(i \sin(\frac{\Omega dt}{2w^2})(b_{0,1}(0)(\Omega + \frac{\delta}{\hbar}w^2) - 2\Omega w^2 a_{0,1}(0)) + b_{0,1}(0)g_d \cos(\frac{\Omega dt}{2w^2}) \right), \quad (\text{A2f})$$

where $\delta = E_{ph} - E_{ex}$ and we introduce:

$$g_c \equiv \sqrt{g^2 + 4\Omega w^2 \frac{\delta}{\hbar} + 4w^4(4\Omega^2 + (\frac{\delta}{\hbar})^2)}, \quad (\text{A3a})$$

$$g_d \equiv \sqrt{\Omega^2 + 2\Omega w^2 \frac{\delta}{\hbar} + w^4(4\Omega^2 + (\frac{\delta}{\hbar})^2)}, \quad (\text{A3b})$$

We present in Fig. 6 some examples for variations of

$a_{n,m}$ and $b_{n,m}$ coefficients for two values of $w = 30\xi$ and $w = \xi$. One notes that for $w = 30\xi$, we can safely keep $a_{0,0}$, $a_{0,1}$, and $a_{1,0}$, as they are four orders larger than the other coefficients. However, with $w = \xi$, we need to take into account more terms for the approximation of the solution.

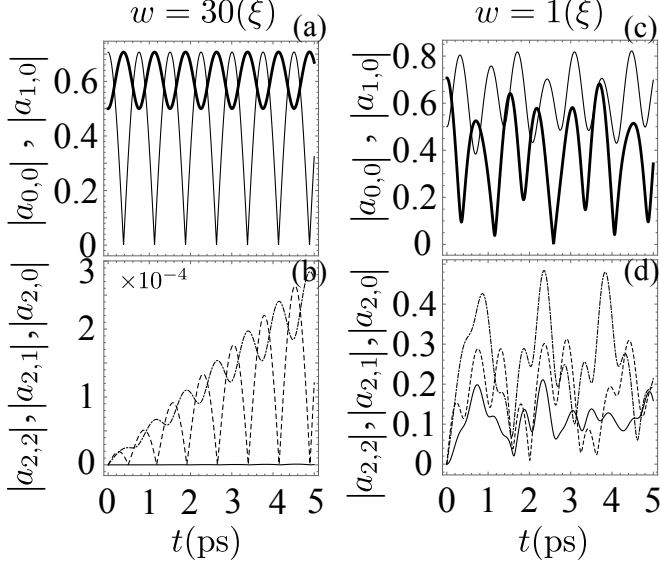


FIG. 6. Variations of $|a_{n,m}|$ with $0 \leq m, n \leq 2$ with respect to time, for two spot sizes of w . For $w = 30\xi$ in the left panels, we can keep $a_{0,0}$ (solid line) and $|a_{1,0}| = |a_{0,1}|$ (thick solid line), while other $a_{n,m}$ are four orders smaller than $a_{0,0}$, $a_{1,0} = a_{0,1}$. It is shown in (b) for $|a_{2,2}|$ (solid line), $|a_{0,2}| = |a_{2,0}|$ (dashed line), and $|a_{1,2}| = |a_{2,1}|$ (dot-dashed line). Right panels show $|a_{n,m}|$ for $w = \xi$, where all coefficients are in the same order.

-
- [1] Daniel Kleppner and Robert Kolenkow, *An Introduction to Classical Mechanics* (Cambridge University Press).
 - [2] P. G. Saffman, *Vortex Dynamics* (Cambridge University Press, 1992).
 - [3] James L. Meriam and L. G. Kraige, *Engineering Mechanics-Dynamics* (Wiley, 2012).
 - [4] Peter R. N. Childs, *Rotating Flow* (Elsevier, 2011).
 - [5] G. Blatter, M. V. Feigel'man, V. B. Geshkenbein, A. I. Larkin, and V. M. Vinokur, "Vortices in high-temperature superconductors," *Rev. Mod. Phys.* **66**, 1125–1388 (1994).
 - [6] A. J. Leggett, "Superfluidity," *Rev. Mod. Phys.* **71**, S318–S323 (1999).
 - [7] M. R. Matthews, B. P. Anderson, P. C. Haljan, D. S. Hall, C. E. Wieman, and E. A. Cornell, "Vortices in a Bose-Einstein Condensate," *Phys. Rev. Lett.* **83**, 2498–2501 (1999).
 - [8] K. G. Lagoudakis, M. Wouters, M. Richard, a. Baas, I. Carusotto, R. André, Le Si Dang, and B. Deveaud-Plédran, "Quantized vortices in an excitonpolariton condensate," *Nat. Phys.* **4**, 706–710 (2008).
 - [9] L. Dominici, D. Colas, A. Gianfrate, A. Rahmani, Carlos S. Muñoz, D. Ballarini, M. De Giorgi, G. Gigli, Fabrice P. Laussy, and D. Sanvitto, "Ultrafast topology shaping by a rabi-oscillating vortex," preprint at <https://arxiv.org/abs/1801.02580> (2018).
 - [10] Alison M. Yao and Miles J. Padgett, "Orbital angular momentum: origins, behavior and applications," *Adv. Opt. Photonics* **3**, 161 (2011).
 - [11] N. S. Voronova, A. A. Elistratov, and Yu. E. Lozovik, "Detuning-controlled internal oscillations in an exciton-polariton condensate," *Phys. Rev. Lett.* **115**, 186402 (2015).
 - [12] Amir Rahmani and Fabrice P. Laussy, "Polaritonic Rabi and Josephson oscillations," *Scientific Reports* **6**, 28930 (2016).
 - [13] Alexey V. Kavokin, Jeremy J. Baumberg, Guillaume Malpuech, and Fabrice P. Laussy, *Microcavities* (Oxford University Press, 2016).
 - [14] M. A. Khomehchi, Khalid Hossain, M. E. Mossman, Yongping Zhang, Th. Busch, Michael McNeil Forbes, and P. Engels, "Negative-mass hydrodynamics in a

- spin-orbit-coupled bose-einstein condensate,” *Phys. Rev. Lett.* **118**, 155301 (2017).
- [15] David Colas, Fabrice P. Laussy, and Matthew J. Davis, “Negative-mass effects in spin-orbit coupled bose-einstein condensates,” *Phys. Rev. Lett.* **121**, 055302 (2018).
- [16] J Kaspzrak, M Richard, S Kundermann, a Baas, P Jeambrun, J M J Keeling, F M Marchetti, M H Szymańska, R André, J L Staehli, V Savona, P B Littlewood, B Deveaud, and Le Si Dang, “Bose-Einstein condensation of exciton polaritons,” *Nature* **443**, 409–414 (2006).
- [17] A. Amo, S Pigeon, D Sanvitto, V G Sala, R Hivet, I Carusotto, F Pisanello, G Leménager, R Houdré, E Giacobino, C Ciuti, and A Bramati, “Polariton superfluids reveal quantum hydrodynamic solitons,” *Science* **332**, 1167–1170 (2011).
- [18] S. Pigeon, I. Carusotto, and C. Ciuti, “Hydrodynamic nucleation of vortices and solitons in a resonantly excited polariton superfluid,” *Phys. Rev. B* **83**, 144513 (2011).
- [19] A. Amo, Jérôme Lefrère, Simon Pigeon, Claire Adrados, Cristiano Ciuti, Iacopo Carusotto, Romuald Houdré, Elisabeth Giacobino, and Alberto Bramati, “Superfluidity of polaritons in semiconductor microcavities,” *Nat. Phys.* **5**, 805–810 (2009).
- [20] M. Abbarchi, A. Amo, V. G. Sala, D. D. Solnyshkov, H. Flayac, L. Ferrier, I. Sagnes, E. Galopin, A. Lemaître, G. Malpuech and J. Bloch, “Macroscopic quantum self-trapping and Josephson oscillations of exciton polaritons,” *Nature* **9**, 275 (2013).
- [21] K. G. Lagoudakis, T. Ostatnický, A. V. Kavokin, Y. G. Rubo, R. André, and B. Deveaud-Plédran, “Observation of half-quantum vortices in an exciton-polariton condensate,” *Science* **326**, 974–976 (2009).
- [22] D. Sanvitto, F. M. Marchetti, M. H. Szymańska, G. Tosi, M. Baudisch, F. P. Laussy, D. N. Krizhanovskii, M. S. Skolnick, L. Marrucci, A. Lemaître, J. Bloch, C. Tejedor, and L. Viña, “Persistent currents and quantized vortices in a polariton superfluid,” *Nat. Phys.* **6**, 527–533 (2010).
- [23] Lorenzo Dominici, Galbadrakh Dagvadorj, Jonathan M. Fellows, Dario Ballarini, Milena De Giorgi, Francesca M. Marchetti, Bruno Piccirillo, Lorenzo Marrucci, Alberto Bramati, Giuseppe Gigli, Marzena H. Szymaska, and Daniele Sanvitto, “Vortex and half-vortex dynamics in a nonlinear spinor quantum fluid,” *Sci. Adv.* **1**, e1500807 (2015).
- [24] Lorenzo Dominici, Ricardo Carretero-Gonzalez, Antonio Gianfrate, Jess Cuevas-Maraver, Augusto S. Rodrigues, Dimitri J. Frantzeskakis, Giovanni Lerario, Dario Ballarini, Milena De Giorgi, Giuseppe Gigli, Panayotis G. Kevrekidis, and Daniele Sanvitto, “Interactions and scattering of quantum vortices in a polariton fluid,” *Nature Communications* **9**, 1467 (2018).
- [25] L. Dominici, D. Colas, S. Donati, J. P. Restrepo Cuartas, M. De Giorgi, D. Ballarini, G. Guirales, J. C. López Carreño, A. Bramati, G. Gigli, E. del Valle, F. P. Laussy, and D. Sanvitto, “Ultrafast control and Rabi oscillations of polaritons,” *Phys. Rev. Lett.* **113**, 226401 (2014).
- [26] D. J. Thouless, Ping Ao, and Qian Niu, “Transverse force on a quantized vortex in a superfluid,” *Phys. Rev. Lett.* **76**, 3758–3761 (1996).
- [27] Ping Ao and David J. Thouless, “Berry’s phase and the magnus force for a vortex line in a superconductor,” *Phys. Rev. Lett.* **70**, 2158–2161 (1993).
- [28] G. D. Mahan, *Many Particle Physics* (Plenum, 2000).
- [29] F. Tassone and Y. Yamamoto, “Exciton-exciton scattering dynamics in a semiconductor microcavity and stimulated scattering into polaritons,” *Phys. Rev. B* **59**, 10830–10842 (1999).
- [30] Yongbao Sun, Yoseob Yoon, Mark Steger, Gangqiang Liu, Loren N. Pfeiffer, Ken West, David W. Snoke, and Keith A. Nelson, *Nature Physics* **13**, 870 (2017).
- [31] Itamar Rosenberg, Dror Liran, Yotam Mazuz-Harpaz, Kenneth West, Loren Pfeiffer, and Ronen Rapaport, “Strongly interacting dipolar-polaritons,” preprint at <https://arxiv.org/abs/1802.01123> (2018).
- [32] William H. Press, Saul A. Teukolsky, William T. Vetterling, and Brian P. Flannery, *Numerical Recipes* (Cambridge University Press, 2007).
- [33] Shijun Liao, *Homotopy Analysis Method in Nonlinear Differential Equations* (Springer, 2012).
- [34] Luca Calderaro, Alexander L. Fetter, Pietro Massignan, and Peter Wittek, “Vortex dynamics in coherently coupled bose-einstein condensates,” *Phys. Rev. A* **95**, 023605 (2017).
- [35] B. Jackson, J. F. McCann, and C. S. Adams, “Vortex line and ring dynamics in trapped bose-einstein condensates,” *Phys. Rev. A* **61**, 013604 (1999).
- [36] Simone Donadello, Simone Serafini, Marek Tylutki, Lev P. Pitaevskii, Franco Dalfovo, Giacomo Lamporesi, and Gabriele Ferrari, “Observation of solitonic vortices in bose-einstein condensates,” *Phys. Rev. Lett.* **113**, 065302 (2014).
- [37] Tian Zhong, Jonathan M. Kindem, John G. Bartholomew, Jake Rochman, Ioana Craiciu, Evan Miyazono, Marco Bettinelli, Enrico Cavalli, Varun Verma, Sae Woo Nam, Francesco Marsili, Matthew D. Shaw, Andrew D. Beyer, and Andrei Faraon, “Nanophotonic rare-earth quantum memory with optically controlled retrieval,” *Science* **357**, 1392–1395 (2017), <http://science.sciencemag.org/content/357/6358/1392.full.pdf>.
- [38] Xuekai Ma, Oleg A. Egorov, and Stefan Schumacher, “Creation and manipulation of stable dark solitons and vortices in microcavity polariton condensates,” *Phys. Rev. Lett.* **118**, 157401 (2017).
- [39] H. Sigurdsson, O. A. Egorov, X. Ma, I. A. Shelykh, and T. C. H. Liew, “Information processing with topologically protected vortex memories in exciton-polariton condensates,” *Phys. Rev. B* **90**, 014504 (2014).
- [40] Jian Wang, Jeng-Yuan Yang, Irfan M. Fazal, Nisar Ahmed, Yan Yan, Hao Huang, Yongxiong Ren, Yang Yue, Samuel Dolinar, Moshe Tur, and Alan E. Willner, “Terabit free-space data transmission employing orbital angular momentum multiplexing,” *Nat. Photon.* **6**, 488–496 (2012).
- [41] I. S. Veshchunov, W. Magrini, A. G. AU Godin, J.-B. Trebbia, A. I. Buzdin, Ph. Tamarat, and B. Lounis, “Optical manipulation of single flux quanta,” *Nature Communications* **7**, 12801 (2016).